

# Plane strain extrusion through curved dies: an upper bound analysis and FEM simulation

Parvaneh amjadian<sup>1\*</sup>

1- Department of Mechanical Engineering, Sahneh Branch, Islamic Azad University, Sahneh, Iran  
\* P.O.B. 6746154973 Sahneh, Iran, [parvaneh.amjadian@gmail.com](mailto:parvaneh.amjadian@gmail.com)

## Abstract

Extrusion is a process used to create objects with uniform cross-sectional profile. A material is pushed through a die of the desired cross-section. In this process, a like other metal forming process, calculating and optimization of the extrusion force is important. Among various methods of solution to metal forming processes, the upper bound technique as an analytical method and finite element method has been widely used for the analysis of the metal forming processes effectively. In this paper, plane strain forward extrusion through an arbitrary die profile was analyzed by upper-bound approach in cylindrical coordinate system and the general velocity field for die with any shape is presented. Deformation zone divided into three deformation zones and the amounts of strain rate in each deformation zone were calculated by exhibiting an admissible velocity field in cylindrical coordinate system. Then, the internal power, the power dissipated on frictional and velocity discontinuity surfaces were obtained and then, the extrusion force and average extrusion pressure was calculated. The extrusion process was simulated by finite element method (FEM). Analytical results were compared with the results given by finite element method (Abaqus software) for curved dies and wedge shaped die. These comparisons showed a good agreement by simulation results. In addition, the effects of various parameters on relative average extrusion pressure were investigated.

## Keywords

Plane strain extrusion, Upper bound, FEM

## 1. INTRODUCTION

Among various methods of solution to metal forming processes, the upper bound technique as an analytical method and finite element method has been widely used for the analysis of the metal forming processes effectively.

A number of people have used the upper bound method to analyze the extrusion process. Avitzur [1] examined axisymmetric extrusion through conical dies using upper bound models. Zimmerman and Avitzur [2] also modeled extrusion using the upper bound method, but with generalized shear boundaries. Chen and Ling [3] developed a velocity field for axisymmetric extrusions through cosine, elliptic and hyperbolic dies. Yang et al. [4] as well as Yang and Han [5] developed upper bound models with streamlined dies. Chen and Ling [6] and Nagpal [7] were among the early investigators who explored alternative die shapes, developing velocity fields for axisymmetric extrusions through arbitrarily shaped dies. Chen et al. [8] and Liu and Chung [9] used finite element analysis to examine axisymmetric extrusion through conical dies. Kim et al. [10] used FEM to design an axisymmetric controlled strain rate die. Gordon et al. were developed the adaptable die design method for axisymmetric extrusion and described them in details in a series of papers [11-13]. Placak et al. [14] developed concept of forming limit curve to investigate forming ability in carbon steel and prediction of central bursting defects. Shebek et al. [15] used numerical simulation by Abaqus/Explicit to investigate of die angle, friction and

reduction ratio effects. They used the uncoupled ductile failure models and compared numerical results with the experimental results. The purpose of this paper is to develop a velocity field that can be used in upper bound method for plane strain extrusion for dies of any shape. The results obtained in upper bound model are compared with finite element method, using the finite element software, ABAQUS.

## 2. UPPER BOUND ANALYSIS

Fig. 1 shows the plane extrusion process parameters in a schematic diagram. To analyse the process by using the upper bound method, the material under deformation is divided into three zones, as shown in Fig. 1.

Zone II is the deformation zone and is surrounded by two cylindrical velocity discontinuity surface  $\Gamma_1$  and  $\Gamma_2$  as well as the die surface. The die surface, which is labelled as  $\psi(r)$  in Fig. 1, is given in the cylindrical coordinate system,  $(r, \theta, z)$  where  $\psi(r)$  is the angular position of the die surface as a function of the radial distance from the origin. The origin of cylindrical coordinate system,  $(r, \theta, z)$ , is located at point  $o$  which is defined by the intersection of the strip midline with a line at angle  $\alpha$  that goes through the point where the die begins and the exit point of the die. The die length is given by the parameter  $L$ . Fig. 1 shows the plane extrusion process parameters in a schematic diagram. The material starts as a strip of thickness  $2t_o$  and is extruded into a strip product of thickness  $2t_f$  through a curved die with length  $L$ . The

material is assumed to be a perfectly plastic material with flow strength  $\sigma_0$ .

To analyze the process by using the upper bound method, the material under deformation is divided into three zones, as shown in Fig. 1. In zones I and III the material moves rigidly with the velocity  $v_o$  and  $v_f$ , respectively. Zone II is the deformation zone and is surrounded by two cylindrical velocity discontinuity surfaces  $\Gamma_1$  and  $\Gamma_2$  as well as the die surface. The die surface, which is labeled as  $\psi(r)$  in Fig. 1, is given in the cylindrical coordinate system,  $(r, \theta, z)$  where  $\psi(r)$  is the angular position of the die surface as a function of the radial distance from the origin.

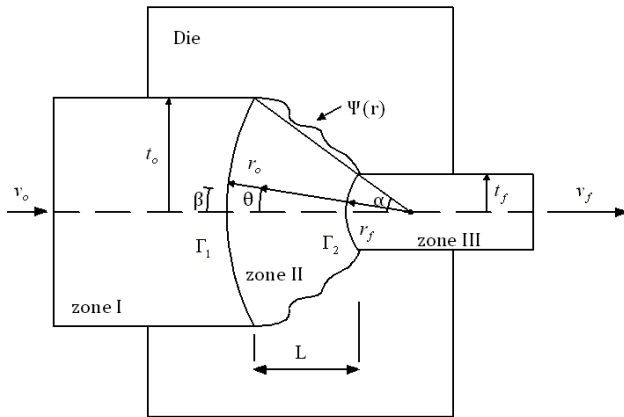


Fig. 1. Schematic diagram of plane strain extrusion to show the derivation of the velocity field.

### 2.1 Velocity field in the deformation zone

The velocity component in the radial direction within the deformation zone  $\dot{U}_r$  can be obtained by assuming volume flow balance. In Fig. 1, the volume flow of material across the  $\Gamma_1$  surface at the point  $(r_o, \beta, z)$ , in the radial direction is

$$dQ = -v_o \cos \beta r_o l d\beta \quad (1)$$

The volume flow of material in the radial direction at the point  $(r, \theta, z)$  in the deformation zone is

$$dQ = \dot{U}_r r l d\theta \quad (2)$$

By equating “(1)” and “(2)”, the radial velocity in the deformation zone is

$$\dot{U}_r = -v_o \frac{r_o}{r} \cos \beta \frac{d\beta}{d\theta} \quad (3)$$

If the assumption of proportional angles in the deformation zone is made, this assumption was used by Gordon et al. [12] for axisymmetric extrusion, then

$$\beta = \frac{\theta \alpha}{\psi} \quad (4)$$

Replacing “(4)” into “(3)” gives the radial velocity component as

$$\dot{U}_r = -v_o \frac{r_o}{r} \frac{\alpha}{\psi} \cos \left( \frac{\theta \alpha}{\psi} \right) \quad (5)$$

The full velocity field for the flow of the material in deformation zone II is obtained by invoking volume constancy. Volume constancy in cylindrical coordinate system is defined as

$$\dot{\epsilon}_{rr} + \dot{\epsilon}_{\theta\theta} + \dot{\epsilon}_{zz} = 0 \quad (6)$$

And strain rates in cylindrical coordinate system is defined as

$$\begin{aligned} \dot{\epsilon}_{rr} &= \frac{\partial \dot{U}_r}{\partial r} \\ \dot{\epsilon}_{\theta\theta} &= \frac{1}{r} \frac{\partial \dot{U}_\theta}{\partial \theta} + \frac{\dot{U}_r}{r} \\ \dot{\epsilon}_{zz} &= \frac{\partial \dot{U}_z}{\partial z} \end{aligned} \quad (7)$$

For the plane strain extrusion (i.e.  $\dot{U}_z = 0$ ) and a full velocity field is obtained by placing  $\dot{U}_r$ , from “(5)” into “(7)”, then radial velocity component becomes as

$$\begin{aligned} \dot{U}_r &= -v_o \frac{r_o}{r} \frac{\alpha}{\psi} \cos \frac{\theta \alpha}{\psi} \\ \dot{U}_\theta &= -v_o r_o \frac{\alpha \theta}{\psi^2} \frac{\partial \psi}{\partial r} \cos \frac{\theta \alpha}{\psi} \\ \dot{U}_z &= 0 \end{aligned} \quad (8)$$

With the strain rate field, and the velocity field, the standard upper bound method can be implemented. This upper bound method involves calculating the internal power of deformation over the deformation zone volume, calculating the shear power losses over the two surfaces of velocity discontinuity, and the frictional power losses between the material and the die.

### 2.2 Shear power losses

The equation for the power losses along a shear surface of velocity discontinuity in an upper bound model is

$$\dot{W}_S = \frac{\sigma_0}{\sqrt{3}} \int |\Delta v| dS \quad (9)$$

So, the shear power losses along the surfaces of velocity discontinuity  $\Gamma_1$  become

$$\dot{W}_{S\Gamma_1} = \frac{\sigma_0}{\sqrt{3}} l v_o r_o \int_0^\alpha \left[ r_o \frac{\partial \psi}{\partial r} \frac{\theta}{\alpha} \cos \theta + \sin \theta \right]_{r=r_o} d\theta \quad (10)$$

The shear power losses along the surface of velocity discontinuity  $\Gamma_2$  become

$$\dot{W}_{S\Gamma_2} = \frac{\sigma_0}{\sqrt{3}} l v_o r_o r_f \int_0^\alpha \left[ \frac{\partial \psi}{\partial r} \frac{\theta}{\alpha} \cos \theta + \frac{\sin \theta}{r_f} \right]_{r=r_f} d\theta \quad (11)$$

### 2.3 Internal power of deformation

The internal power of deformation for a perfectly plastic material with flow stress of  $\sigma_0$  in an upper bound model is

$$\dot{W}_i = \frac{2}{\sqrt{3}} \sigma_0 \int \sqrt{\frac{1}{2} \dot{\epsilon}_{ij} \dot{\epsilon}_{ij}} dV \quad (12)$$

So, internal power of deformation become

$$\dot{W}_i = \sqrt{\frac{2}{3}} \sigma_0 l v_0 r_o \int_0^\psi \int_{r_f}^{r_o} \left[ \frac{2 \alpha^2}{r^2 \psi^2} (A)^2 + \frac{1 \alpha^2}{4 \psi^4} (B)^2 \right]^{1/2} r d\theta dr$$

$$A = \frac{1}{r} \cos \frac{\theta \alpha}{\psi} + \frac{1}{\psi} \frac{\partial \psi}{\partial r} \cos \frac{\theta \alpha}{\psi} - \frac{\theta \alpha}{\psi^2} \frac{\partial \psi}{\partial r} \sin \frac{\theta \alpha}{\psi}$$

$$B = \frac{\alpha}{r^2} \sin \frac{\theta \alpha}{\psi} + \frac{\theta}{r} \frac{\partial \psi}{\partial r} \cos \frac{\theta \alpha}{\psi} - \theta \frac{\partial^2 \psi}{\partial r^2} \cos \frac{\theta \alpha}{\psi} - \frac{\theta^2 \alpha}{\psi^2} \left( \frac{\partial \psi}{\partial r} \right)^2 \sin \frac{\theta \alpha}{\psi} - \frac{2\theta}{\psi} \left( \frac{\partial \psi}{\partial r} \right)^2 \cos \frac{\theta \alpha}{\psi} \quad (13)$$

#### 2.4 Friction power losses

The general equation for the friction power losses for a surface with a constant friction factor is

$$\dot{W}_f = \frac{\sigma_0}{\sqrt{3}} m_f \int |\Delta v| dS \quad (14)$$

Where  $m_f$  is the constant friction factor, and

$$|\Delta v| = \dot{U}_r \cos \eta + \dot{U}_\theta \sin \eta \Big|_{\theta=\psi}$$

The friction power losses along the die surface is calculated as

$$\dot{W}_{f1} = \frac{\sigma_0}{\sqrt{3}} m_f l v_0 r_o \cos \alpha \int_{r_f}^{r_o} \frac{\alpha}{\psi} \left[ \frac{1}{r} + \frac{r r_o}{t_o} \left( \frac{\partial \psi}{\partial r} \right)^2 \right] \frac{1}{\sqrt{\left( \frac{r}{t_o} \right)^2 \left( r_o \frac{\partial \psi}{\partial r} \right)^2 + 1}} dr \quad (15)$$

The friction power losses along the die surface in the deformation zone I can be given by

$$\dot{W}_{f2} = \frac{\sigma_0}{\sqrt{3}} m_f l v_0 (L_o - x) \quad (16)$$

Where  $x$  is displacement of the punch and  $L_o$  is the initial strip length.

The externally supplied pressure, for plane strain extrusion is

$$p_{ave} = \frac{J^*}{2 t_o l v_0} \quad (17)$$

By the upper bound model, the externally supplied power is less than or equal to the sum of the powers described in “(10)”, “(11)”, “(13)”, “(15)” and “(16)”.

If one assumes the equality, then the total power is

$$J^* = 2 \times (\dot{W}_{S_{r1}} + \dot{W}_{S_{\theta1}} + \dot{W}_i + \dot{W}_{f1} + \dot{W}_{f2}) \quad (18)$$

This upper bound equation includes a parameter  $L$ , length of the die, to be optimized.

### 3. RESULTS AND DISCUSSION

The developed velocity field and upper bound model can be used for plane strain extrusion through dies of any shape if the die profile is expressed as equation  $\psi(r)$ . The die shape of Yang and Han [6, 7] is selected. They created a streamlined die shape as a fourth-order polynomial whose slope is parallel to the axis at both entrance and exit. The equation  $\psi(r)$  describing the die shape of Yang and Han was expressed by Ref. [4].

The initial strip was aluminum with the flow stress as  $\sigma = 189.2 \varepsilon^{0.239} MPa$  and an average of the flow stress is used in analysis.

Fig. 2 shows the relative average extrusion pressure calculated as a function of the die length. Fig. 3 shows the relative average extrusion pressure calculated as a function of the die length in there constant friction factor. By increase constant friction factor, the optimums die length is decreased. Fig. 4 shows the effect of reduction of the cross-sectional area on optimum die length in .By increase reduction of the cross-sectional area, the optimums die length is increased.

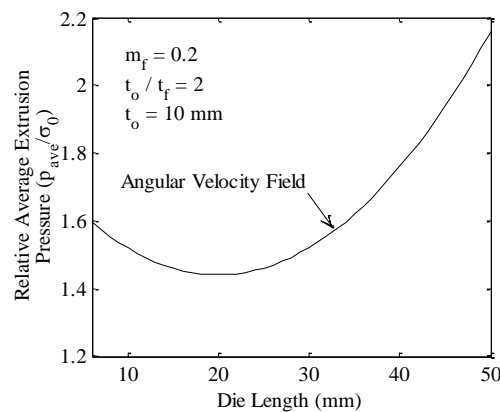


Fig. 2. Relative extrusion pressures for extrusion through Yang and Han die shape.

### 3. FINITE ELEMENT SIMULATION

The plane strain extrusion processes have been simulated using the finite element software, ABAQUS. Due to the symmetry of the process, the finite element meshes are generated on the half cross-section of the strip. In Fig. 5, the average extrusion pressure curves obtained from the upper bound solution and the FEM simulation are

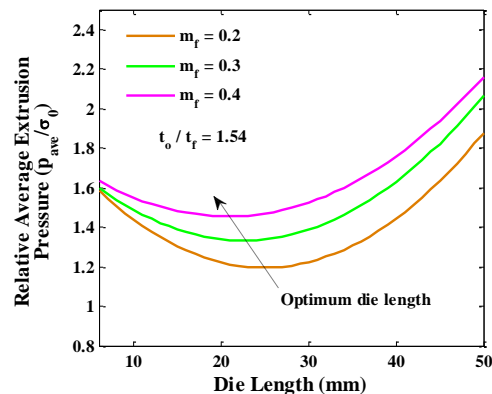
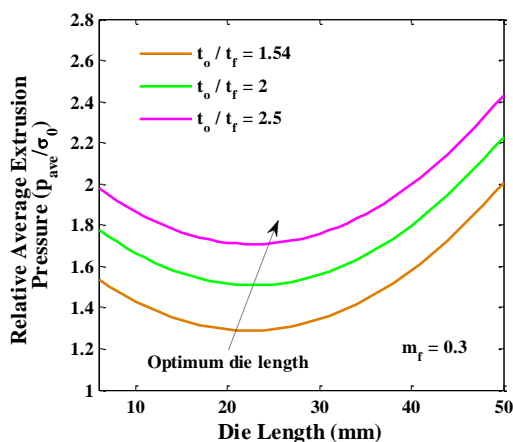


Fig. 3. Effects of constant friction factor on optimums die length.



**Fig. 4.** Effects of reduction of the cross-sectional area on optimum die length

compared with each other. As shown in this figure, the results show good agreement between the analyses and FEM results. The analytically predicted extrusion forces are higher than the FEM results, which is due to the nature of the upper bound.

#### 4. CONCLUSIONS

In this paper a velocity field and their power terms for plane strain extrusion through curved dies was presented. Extrusion force for plane strain extrusion through a curved die was obtained from the upper bound method. The corresponding results have also been determined by using the finite element code and compared with analytical results. These comparisons showed a good agreement.

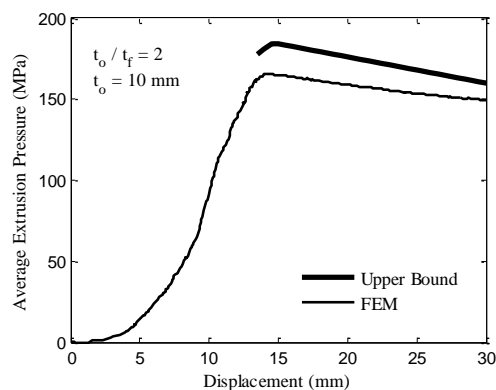


**Fig. 5.** Comparison of analytical, FEM force-displacement curves for Yang & Han die shape.

#### 6. REFERENCES

[1] B. Avitzur, "Metal forming: processes and analysis" New York, McGraw-Hill, 1968.

[2] Z. Zimmerman Z., B. Avitzur, ASME "Journal of Engineering for Industry" 1970, p.119. Vol. 92.  
 [3] C.T. Chen and E.F. Ling, "International Journal of Mechanical Sciences" Vol. 1968, p. 863.  
 [4] D.Y. Yang, C.H. Han, B.C. Lee, "International Journal of Mechanical Sciences" Vol. 27.1985, p. 653.  
 [5] D.Y. Yang and C.H. Han, "ASME Journal of Engineering for Industry" Vol 109, 1987, p.161.  
 [6] C.T. Chen, F.F. Ling, "International Journal of Mechanical Sciences" Vol. 10, 1968, p. 863.  
 [7] V. Nagpal, "ASME Journal of Engineering for Industry" Vol. 96, 1974, p.1197.  
 [8] C.C. Chen, S.I. Oh and S. Kobayashi, "ASME Journal of Engineering for Industry" Vol. 101, 1979, p. 23.  
 [9] T.S. Liu T.S., N.L. Chung N.L., "Extrusion analysis and workability prediction using finite element method", Computers and Structures Vol. 36 ,1990, p. 369.  
 [10] N.H. Kim, C.G. Kang and B.M. Kim, "Die design optimization for axisymmetric hot extrusion of metal matrix composites", International Journal of Mechanical Sciences Vol. 43, 2001, p.1507.  
 [11] W.A. Gordon, C.J. Van Tyne and Y.H. Moon, "International Journal of Mechanical Sciences" Vol. 49, 2007, p. 86.  
 [12] W.A. Gordon, C.J. Van Tyne and Y.H. Moon, "International Journal of Mechanical Sciences" Vol. 49, 2007. p. 96.  
 [13] W.A. Gordon, C.J. Van Tyne, Y.H. Moon, International Journal of Mechanical Sciences Vol. 49,2007, p. 104.  
 [14] Plancak M, Vilotic D, Kacmarcik I, "Stress state in forward cold extrusion". Journal for Technology of Plasticity, 2014, 39: 21-27.  
 [15] Sebeka F, Kubik P, Petruska J, "Prediction of central bursting in the process forward extrusion using the uncoupled ductile failure models". Advances in Materials and Processing Technologies, 2015, 1: 43-48.